Microstructure Evolution and Tensile Properties of Zr-2.5wt%Nb Pressure Tubes Processed from Billets with Different Microstructures

K. Kapoor, K. Muralidharan, and N. Saratchandran

(Submitted 24 December 1997; in revised form 15 September 1998)

Starting with identical ingots, billets having different microstructures were obtained by three different processing methods for fabrication of Zr-2.5wt%Nb pressure tubes. The billets were further processed by hot extrusion and cold Pilger tube reducing to the finished product. Microstructural characterization was done at each stage of processing. The effects of the initial billet microstructure on the intermediate and final microstructure and mechanical property results were determined. It was found that the structure at each stage and the final mechanical properties depend strongly on the initial billet microstructure. The structure at the final stage consists of elongated alpha zirconium grains with a network of metastable beta zirconium phase. Some of this metastable phase transforms into stable beta niobium during thermomechanical processing. Billets with quenched structure resulted in less beta niobium at the final stage. The air cooled billets resulted in a large amount of beta niobium. The tensile properties, especially the percentage elongation, were found to vary for the different methods. Higher percentage elongation was observed for billets having quenched structure. Extrusion and forging did not produce any characteristic differences in the properties. The results were used to select a process flow sheet which yields the desired mechanical properties with suitable microstructure in the final product.

Keywords alpha zirconium, beta niobium, beta zirconium, extrusion, heat treatment, percentage elongation, Pilger tube reducing, Zr-2.5%Nb

1. Introduction

Pressurized heavy water reactors (PHWR) use zirconium-base alloys for their low neutron-absorption cross section, good mechanical strength, low irradiation creep, and high corrosion resistance in reactor atmospheres. Zr-2.5wt%Nb alloy currently used for pressure tubes has proved more suitable than Zircaloy-2 due to comparatively lower deutrium pickup rate, higher mechanical strength, and better in-reactor creep and corrosion resistance properties (Ref 1). Good mechanical strength and high ductility at reactor operating temperature are essential design features for this material.

The fabrication method for manufacture of Zr-2.5wt%Nb pressure tubes includes water quenching of billets preheated to 1000 °C (beta range); this step is also known as beta quenching. This is done for randomization of texture, homogenization of chemical composition, and refinement of grain structure. The present studies were focused on explaining the differences, if any, in the microstructure at various stages and the tensile properties at the final stage when different processing methods were used for billet manufacture.

K. Kapoor and **N. Saratchandran,** Quality Assurance Group (NDT), Nuclear Fuel Complex, Hyderabad 500 062, India; and **K. Muralidharan,** Defense Metallurgical Research Laboratory, Hyderabad, India. Contact e-mail: sarat@nfc.ernet.in.

2. Experimental and Process Details

Table 1 shows typical chemical composition of the material. The chemistry of all the tubes was similar. Product analysis of each tube was within the chemical specification mentioned in the table. Hydrogen and trace elements like chlorine and phosphorous have been limited to lower values in recent specifications. This improves the in-reactor performance of the tubes while other properties (microstructure, tensile, corrosion, etc.) are likely to be unchanged. Although the material in the present study conformed to an earlier specification, the results of the present study were not affected by these changes.

The three processing methods used to manufacture the tubes in this study are shown in Table 2. In method 1, the ingots were hot extruded to billet size (230 mm diameter) and then beta

Table 1 Typical chemical analysis of Zr-2.5%Nb pressure-tube material

	Composition		
	Specified		
Element	Old	Revised	By analysis
Niobium,%	2.4-2.8	2.4-2.8	2.6
Oxygen, ppm	900-1300	900-1300	1148
Iron, ppm	1500 max	650 max	1160
Chromium, ppm	200 max	200 max	150
Tin, ppm	100 max	50 max	<25
Copper, ppm	30 max	30 max	<30
Nitrogen, ppm	65 max	65 max	30
Hydrogen, ppm	25 max	5 max	<10
Chlorine, ppm	…	0.5 max	…
Phosphorous, ppm	…	10 max	…
Zirconium, ppm	bal	bal	bal

quenched. This is the standard processing method used presently. In method 2, the ingots were hot forged to an intermediate size and then beta quenched. These were finally reduced to billet size by a second hot forging. Method 3 is identical to method 2, except for an additional beta quenching step after the second hot forging. Optical and transmission electron microscopy (TEM) was carried out at this billet stage (stage 1). The processing methods 1, 2, and 3 hereafter were identical.

Billets from these three methods were hot extruded in a similar way by preheating to 800 °C and by extruding through a conical die to hollow blanks that were cooled subsequently and slowly in air. Microstructure evaluations on samples collected after extrusion (stage 2) from the three processing methods were done using scanning electron microscopy (SEM) to examine backscatter images. These extruded hollow blanks were stress relieved at 480 °C for 3 h and cold reduced by Pilger tube reducing in two stages with an intermediate annealing at 550 °C for 6 h. The first cold reduction was limited to approximately 60% and the second cold reduction was limited to approximately 22%. A length of 110 mm was cut from each tube for tensile testing and structure evaluation after the second pilgering. The piece was stress relieved in a muffle furnace at 400 °C for 36 h.

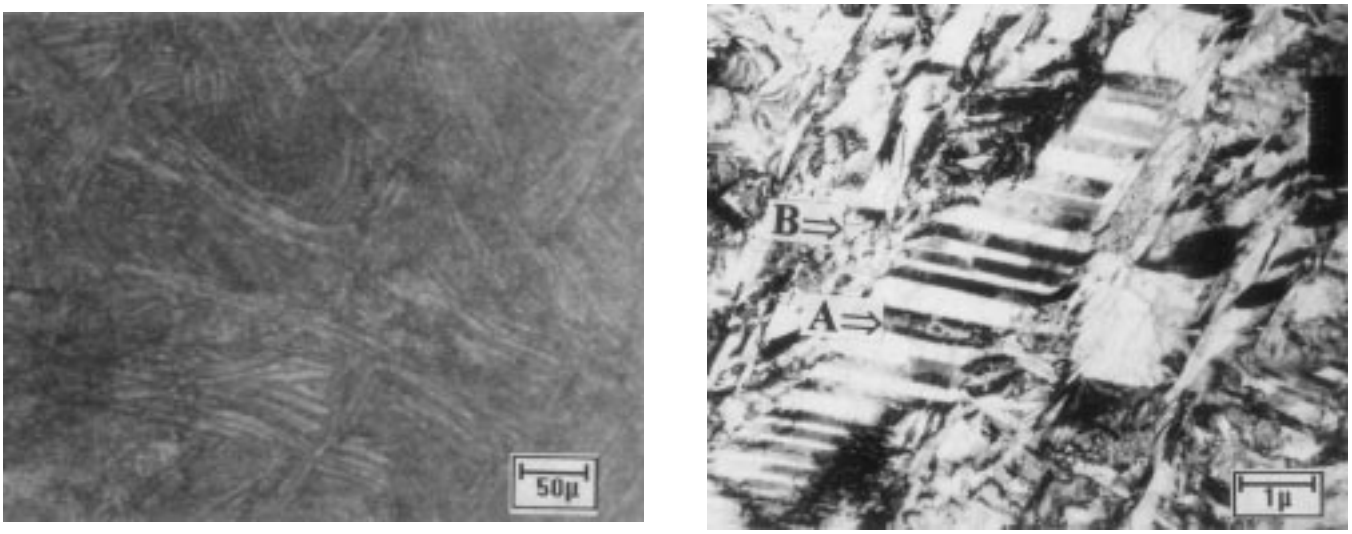

(a) **(b)**

Fig. 1 Billet microstructure for processing method 1 taken at stage 1. (a) Optical micrograph showing martensitic structure. (b) TEM structure showing a twinned primary martensitic plate, A, surrounded by secondary martensite, B

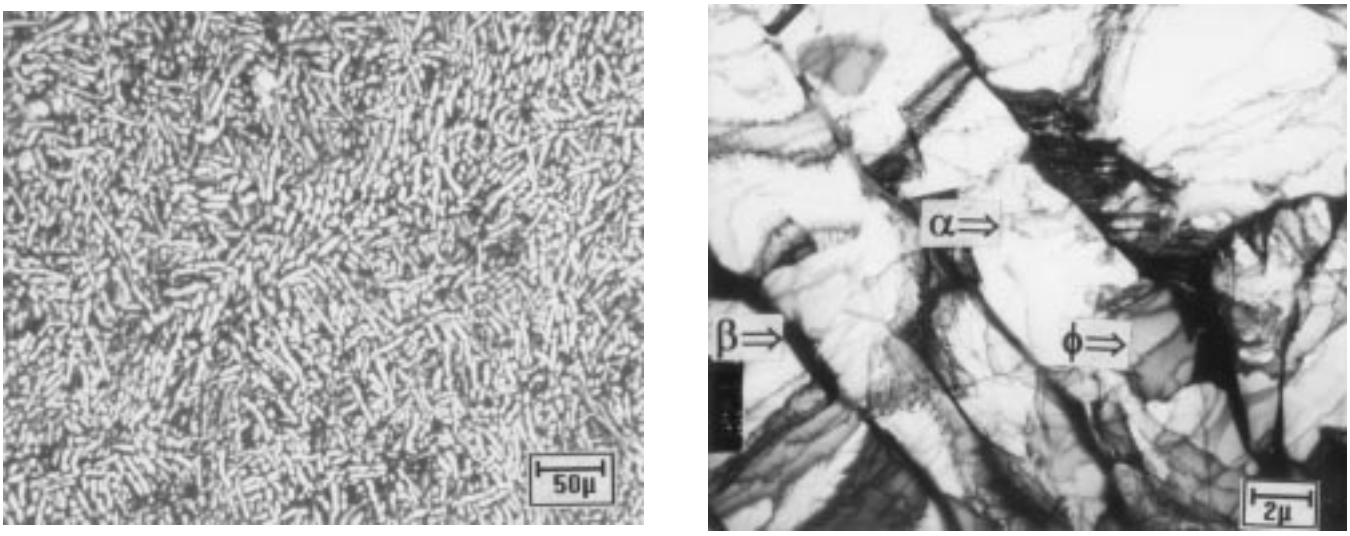

(a) **(b)**

Fig. 2 Billet microstructure for processing method 2 taken at stage 1. (a) Optical micrograph showing air-cooled two-phase structure. (b) TEM structure showing light alpha zirconium grains, α, containing dislocation network, ϕ, surrounded by a film of dark beta zirconium phase, β

Cold working in two steps with an intermediate anneal produces tubes with certain advantages over those produced from a single cold work of 22 to 25% after extrusion (the route followed elsewhere, Ref 2 and 3). The two-stage reduction with an intermediate anneal resulted in a smaller aspect ratio of alpha and beta grains leading to improved reactor performance (Ref 4). Samples for optical and transmission electron microscopy (TEM) were collected at the final stage (stage 3). Optical metallographic samples were etched using HF + HNO_3 + H_2O solution. Thin foils for TEM were prepared by electropolishing using double-jet thinning in a solution of 6% sulfuric acid in methanol maintained at –50 °C. Thin foils were examined in a PEM430T (Philips Electron Instruments Corporation, Mahwah, NJ) TEM operating at 300 kV.

Tensile properties were evaluated from samples taken from the axial direction of the tubes. These were tested on an Instron 1185 universal testing machine (Instron Corporation, Canton, MA) at 300 ° C as per ASTM E 21.

3. Results

Optical and electron micrographs of samples taken at stage 1 from methods 1, 2, and 3 are shown in Fig. 1, 2, and 3, respectively. Fine acicular martensitic structures with a basket weave pattern are seen in the optical micrograph, Fig. 1(a) and 3(a), taken at billet stage from processing methods 1 and 3, respectively. The corresponding structures under TEM show as plates of martensite (Fig. 1b and 3b). A twinned primary martensitic plate (marked "A") surrounded by secondary martensite (marked "B") is seen in Fig. 1b (Ref 5). The sample from processing method 2 taken at stage 1 under optical microscope reveals a two-phase structure consisting of (light) alpha phase surrounded by (dark) beta phase (Fig. 2a). The corresponding TEM structure shows clear alpha- and beta-phase separation (Fig. 2b). The beta phase is present as a thin film surrounding the alpha grains. A fine dislocation network inside alpha grains is also observed. This is a typical slowly cooled structure for this alloy.

The resulting microstructures after extrusion (stage 2) as seen in the SEM are shown in Fig. 4 . The dark regions represent the alpha phase, while thin, elongated, light stringers represent the beta phase. The structure resulting from processing method 1 (Fig. 4a) exhibits beta stringers relatively distinctly and evenly spaced while those from processing methods 2 and 3 (Fig. 4b, c) are broken, varying in thickness and spacing. It is difficult to quantify the structures, especially those from processing methods 2 and 3, due to nonuniform beta-phase distribution.

At stage 3, the material is in a cold-worked state. The optical structures at this stage do not reveal any details due to cold work and fine grain structure.

Figures 5 to 7 are the TEM resulting from processing methods 1, 2, and 3 at stage 3, respectively. Figure 5(a) shows the

Table 2 Three processing methods with different billet-process schedules for manufacture of Zr-2.5%Nb pressure tubes

Processing method	Billet-process schedules
1	Ingot
	Hot extrusion to billet
	Beta quench at 1000 °C
2	Ingot
	Hot forging to intermediate size
	Beta quench at 1000 °C
	Hot forging to billet at 850 °C (air cool)
3	Ingot
	Hot forging to intermediate size
	Beta quench at 1000 °C
	Hot forging to billet at 850 °C (air cool)
	Beta quench at 1000 °C

Note: After initial processing, a stage 1 sample was taken. All three methods then proceeded as follows. Stage 2: hot extrusion at 800 °C to blanks followed by stress relieving at 480 °C for 3 h; Stage 2 sample collected. Stage 3: first pass Pilger tube reducing (60% cold work), stress relieving at 550 °C for 6 h, second pass Pilger tube reducing process (22% cold work) , and stress relieving at 400 °C for 36 h; Stage 3 sample collected

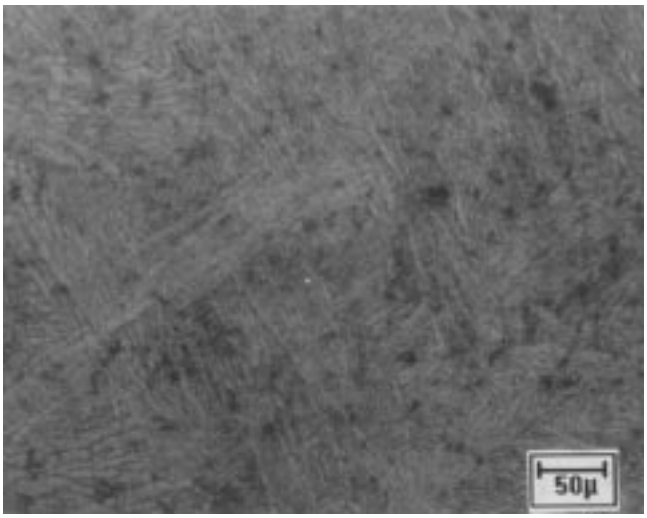

(a)

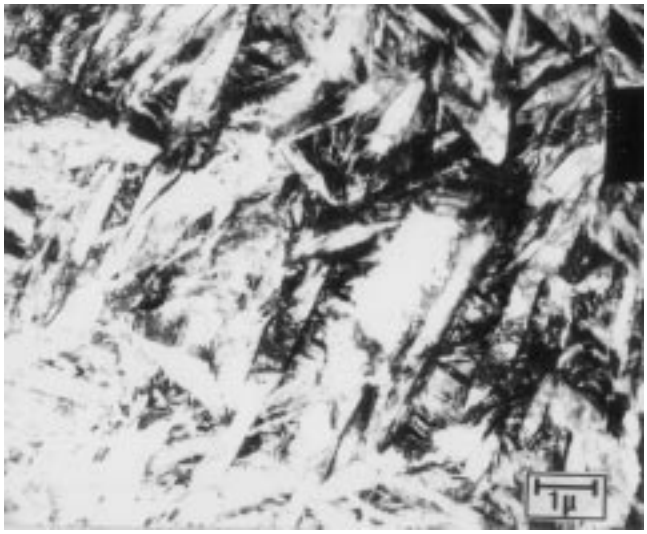

(b)

Fig. 3 Billet microstructure for processing method 3 at stage 1. (a) Optical micrograph. (b) TEM similar to Fig. 1

presence of elongated alpha grains oriented in the working direction. Figure 5(b) shows a selected area diffraction (SAD) pattern from [11$\bar{2}$0] plane from alpha zirconium. During processing of this material, the various heat treatments (intermediate annealing and final stress relieving) result in the dissociation of phases of beta-zirconium (present in extruded blank stage) to stable beta-niobium and alpha-zirconium phases (Ref 6, 7). Figure 5(c) shows SAD from [111] plane of a beta-niobium precipitate. The number of precipitates in this case is few. Figure 6(a) is from a sample taken at stage 3 from processing method 2. This micrograph reveals the presence of a large number of globular precipitates at the grain boundary of alpha zirconium. SAD from [11$\bar{2}$0] plane from alpha zirconium is shown in Fig. 6(b). Figure 6(c) shows SAD from [100] plane of beta-niobium precipitate at the grain boundary.

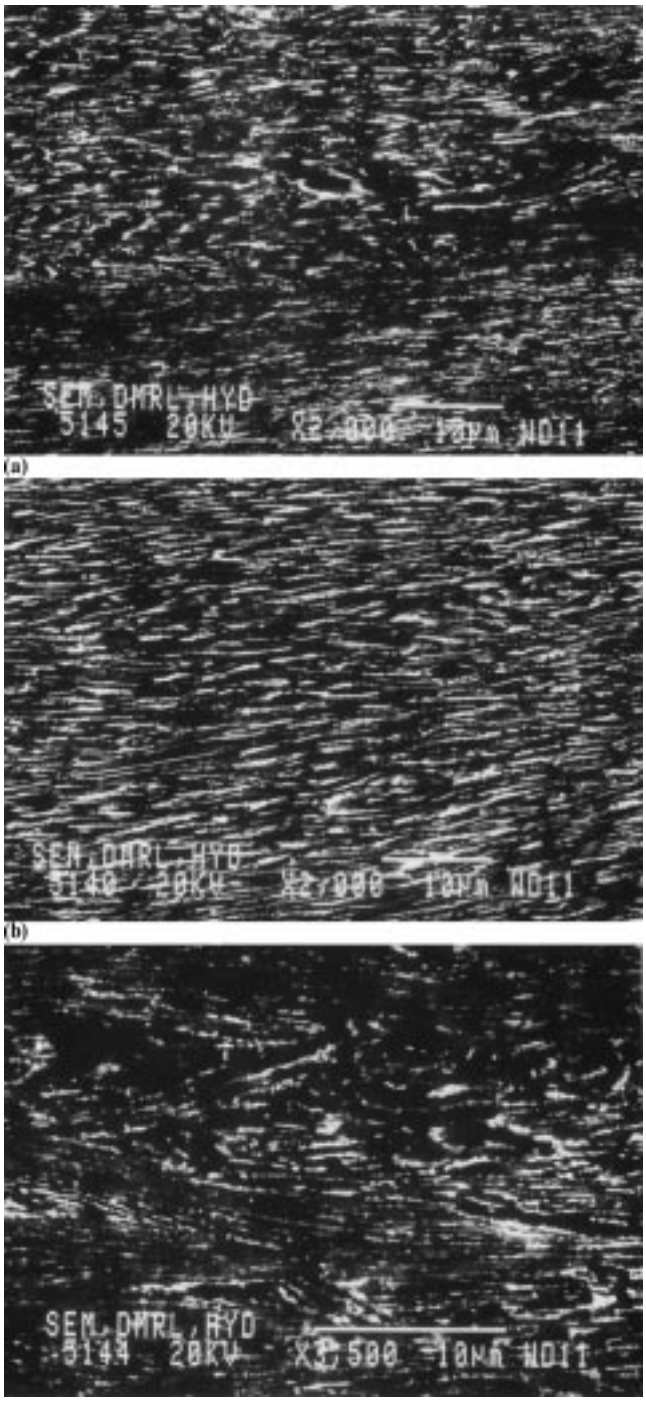

(c)

Fig. 4 Microstructure of as extruded material at stage 2. Back scatter SEM image showing a two-phase structure containing thin, light-colored beta phase. (a) Processing method 1. (b) Processing method 2. (c) Processing method 3

Figure 7(a) is from a sample taken at stage 3 from processing method 3; it reveals elongated alpha-zirconium grains with some beta-niobium precipitates at the alpha grain boundaries. The number of precipitates is similar to that observed for processing method 1. SAD from alpha-zirconium and beta-niobium are shown in Fig. 7(b) and (c), respectively. Figure 8 shows statistical distribution of tensile properties evaluated at 300 °C. Each set of data from the three different process routes consist of results from more than 160 tubes. It is observed that the percentage of tubes having ultimate tensile strength (UTS) greater than 520 MPa in processing methods 1, 2, and 3 are 67, 75, and 70%, respectively. A similar trend is observed for 0.2% yield strength (YS). Bar charts on percentage of elongation show forward skew for processing method 1 (i.e., toward higher percentage elongation) and a backward skew for processing method 2 (i.e., toward lower percentage elongation). The percentages of tubes having elongation greater than 16% in processing methods 1, 2, and 3 are 94, 52, and 82%, respectively. Ductility in the finished stage is highest in processing method 1.

4. Discussion

The structure after extrusion essentially consists of elongated alpha-zirconium with a beta-zirconium phase present as thin stringers along the extrusion direction. During subsequent processing, the effect of various heat treatments is formation of stable beta-niobium from metastable beta-zirconium. One of the major differences in the final microstructure of the tubes from the three processing methods is the quantity and distribution of this niobium rich phase. The quantity of this phase observed in method 2 is much greater than that observed in methods 1 and 3. In process 2, the beta-zirconium phase is already present in the preextrusion stage. During further processing, its dissociation to beta-niobium and alpha-zirconium is quite high. Processes 1 and 3 have quenched (martensitic) structure before extrusion and beta-zirconium is formed only after extrusion to blanks. This results in less beta-niobium in the final stage.

The tensile properties obtained at elevated temperature can be correlated to the structure at the final stage. The presence of these second-phase particles (i.e., beta-niobium precipitates), which are hard and brittle at the grain boundaries, weaken the grain boundaries. This results in the observed loss of ductility as in case of process 2. The effect on strength will be reversed; these precipitates will restrict the movement of dislocations and result in higher strength values.

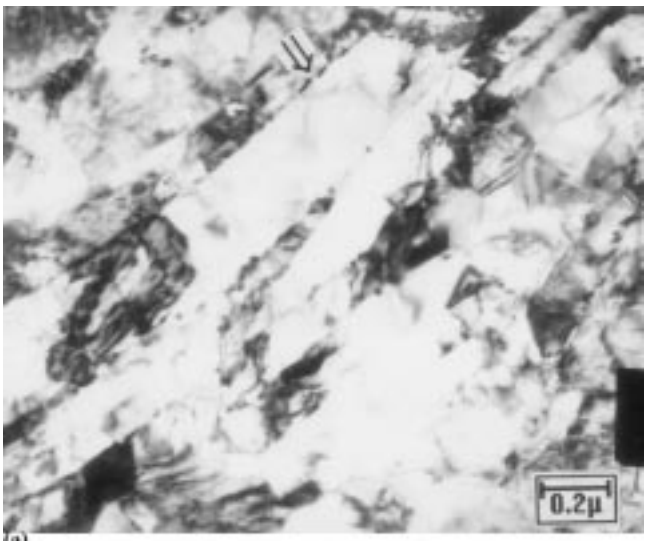

(a)

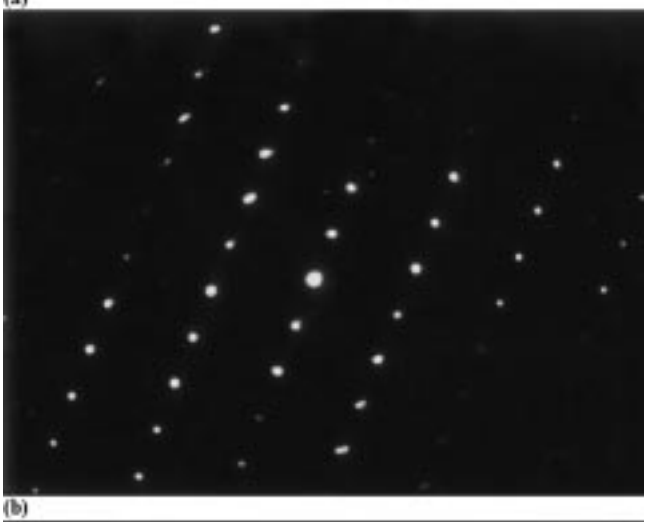

(b)

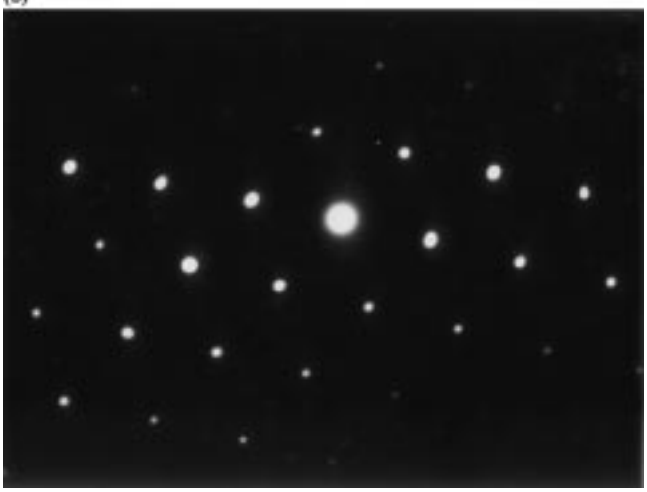

(c)

Fig. 5 (a) Microstructure at finished stage for processing method 1 (stage 3) showing typical bamboo-tree structure with small amount of beta niobium precipitated from beta zirconium phase at alpha phase boundary (see arrow). (b) SAD from alpha zirconium [11$\bar{2}$0] plane. (c) SAD from beta niobium precipitate [111] plane

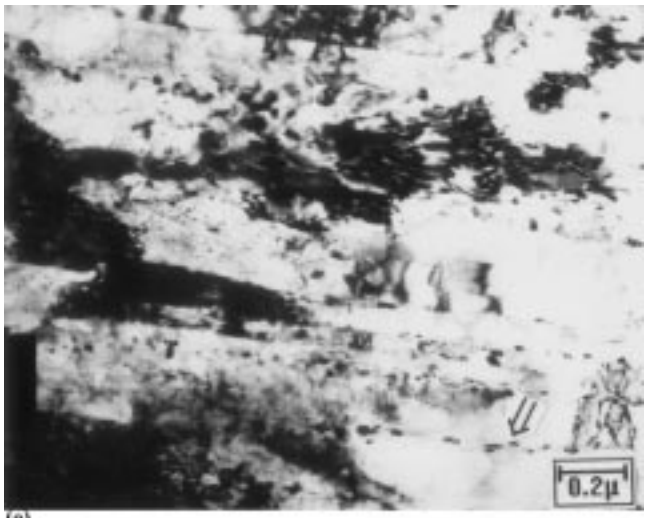

(a)

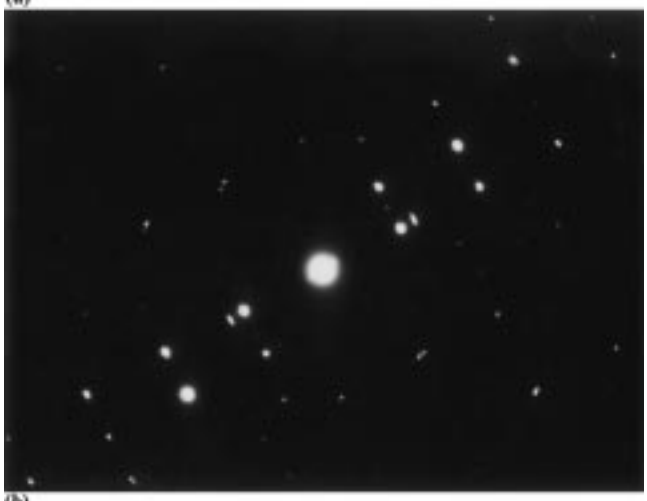

(b)

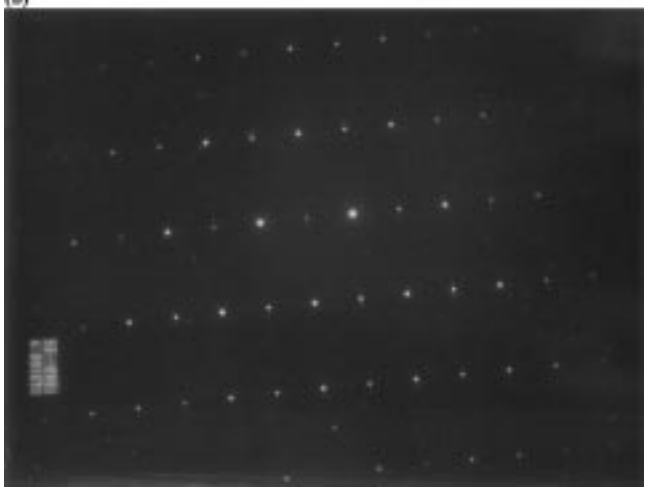

(c)

Fig. 6 Microstructure at finished stage for processing method 2 (stage 3) showing larger amount of beta-niobium precipitated at alpha phase boundary (see arrow). (b) SAD from alpha zirconium [11$\bar{2}$0] phase. (c) SAD from beta-niobium [100] plane

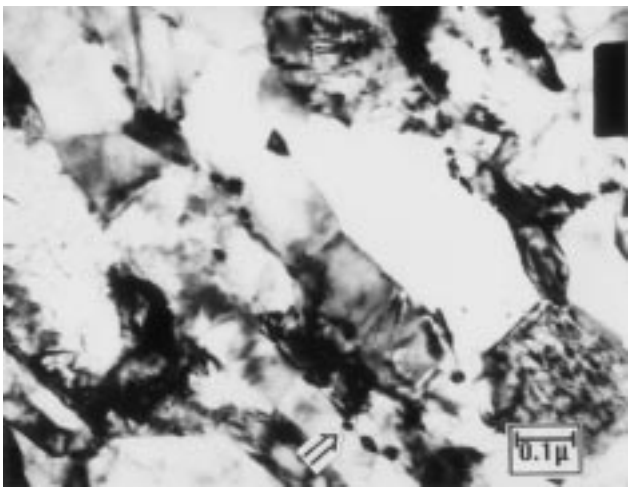

(a)

(b)

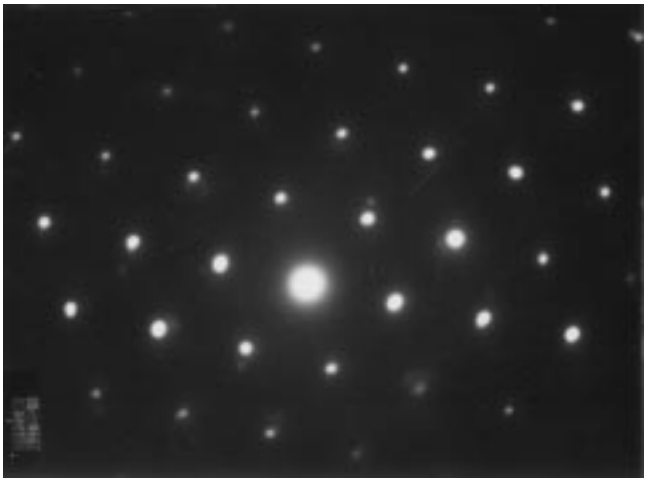

(c)

Fig. 7 (a) Microstructure at finished stage for processing at method 3 (stage 3) showing some beta-niobium precipitate at alpha phase boundary (see arrow). (b) SAD from alpha zirconium [1120] plane. (c) SAD from beta-niobium [111] plane

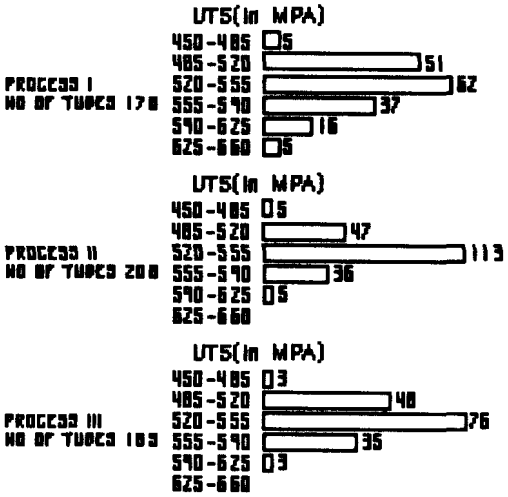

(a)

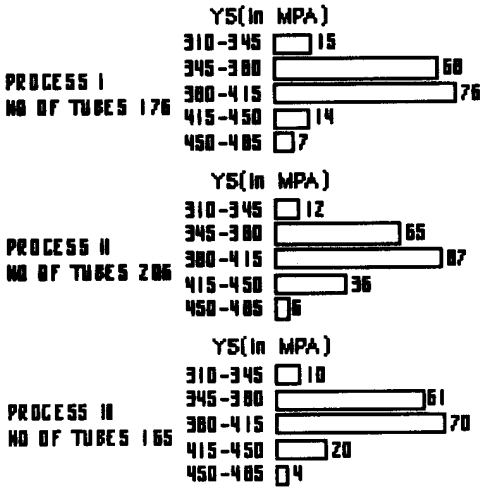

(b)

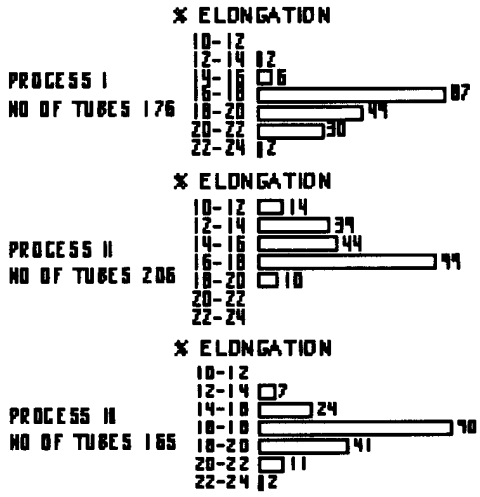

(c)

Fig. 8 Distribution of mechanical properties evaluated at 300 °C at final stage. (a) Ultimate tensile strength. (b) 0.2% yield strength. (c) Percentage elongation

5. Conclusions

The structure and properties of the final product are affected by the process schedule and the condition of billets before extrusion.

During the processing of these tubes, the various heat treatments tend to decompose the metastable beta-zirconium to stable beta-niobium and alpha-zirconium. Thus the grain boundary precipitates of beta-niobium exist in the final structure.

The quantity of this phase depends on the initial structure of the billets before extrusion. Fine acicular martensitic structure before extrusion results in less beta-niobium precipitates in the final structures (processes 1 and 3).

There is a difference in tensile properties (especially percentage of elongation) of the materials processed from different methods that is attributed to the final microstructure, which contains varying amounts of stable beta-niobium.

Acknowledgments

The authors gratefully acknowledge Dr. C. Ganguly and K.K. Sinha, The Nuclear Fuel Complex (NFC), Hyderabad, India, for their encouragement for carrying out this work. The authors also thank D. Banerjee, Defense Metallurgical Research Laboratory (DMRL), Hyderabad, India, for his support.

References

1. W. Evans, O.A. Ross-Ross, J.E. Le Surf, and H.E. Teston, Atomic Energy of Canada Ltd. Report, 2982, 1971
2. B.A. Cheadle, C.E. Coleman, and H. Light, Candu-PHN Pressure Tubes: Their Manufacture, Inspection and Properties, *Nucl. Technol.*, Vol 57, 1982, p 413-424
3. R.G. Fleck, V. Perovic, et al., Development of Modified Pressures Tubes, *Ontario Hydro Research Review*, Vol 8, 1993, p 1-13
4. M.K. Asundi and S. Banerjee, Zirconium Alloys: A Cladding Structural Materials for Water Cooled Reactors, *Mater. Sci. Forum*, Vol 48 and 49, 1989, p 201-220
5. S. Banerjee and R. Krishnan, Martensite Transformation in Zr-Nb Alloys, *Acta Metall.*, Vol 19, 1971, p 1317-1326
6. D.O. Northwood and W.L. Fong, Modification of Structure of Cold Worked Zr-2.5%Nb Nuclear Reactor Pressure Tube Material, *Metallography*, Vol 13, 1980, p 97-115
7. D. Srivastava, G.K. Dey, and S. Banerjee, "Evolution of Microstructure during Fabrication of Zr-2.5%Nb Alloy Pressure Tubes," Bhabha Atomic Research Centre Technical Report, I/011, 1992